JOURNAL OF THEORETICAL AND APPLIED MECHANICS
47, 2, pp. 343-362, Warsaw 2009

A GYROSCOPE-BASED SYSTEM FOR LOCATING A POINT SOURCE OF LOW-FREQUENCY ELECTROMAGNETIC RADIATION

Zbigniew Koruba
Janusz Tuśnio

Kielce University of Technology, Kielce, Poland

e-mail: ksmzko@tu.kielce.pl

The work discusses a new concept of locating the angular position of an electromagnetic radiation source. It presents a mathematical model and calculations concerning the process of target location. The considerations include the guidance of aerial vehicles onto targets of this type.

Key words: gyroscope based system, sensors, electromagnetic radiation, location of position

1. Introduction

Modern civilizations make use of various forms of energy. The most common, however, is the electric energy. After being generated in industrial facilities, it is transmitted and distributed over long distances by means of overhead high- and medium-voltage power lines. It needs to be stepped down several times until it reaches end-users. Because of little visibility and considerable geometrical dimensions (Figs. 1 and 2), power lines may constitute a threat to low–flying vehicles such as motor hang gliders, small planes, etc. (Fig. 3) even during peace time. Under warfare conditions, power lines are strategically important targets, especially for the air force. They are distroyed or temporarily disabled to paralyse industrial production and other economic activities.

From the above considerations, it is clear that accurate and reliable measurement systems are necessary for detecting and locating power lines and similar objects. The operations require determining the exact distance from the target and its angular position early enough to avoid a collision or, during military missions, to perform a successful attack if missiles, aerial cluster bombs or unmanned aerial vehicles are used.

Fig. 1. 500 kV-powerline section running over theYangtze River (the People's Republic of China)

Fig. 2. A rescue helicopter flying dangerously close to a power line (Monsoo Park, 2003)

Whether a transmission line is to be attacked or omitted by an approaching flying object, it is essential that the operations of target/obstacle detection, location and then flying object guidance be performed with high precision.

Most aerial vehicles used for civilian and military purposes fly at very high velocities and their maneuvering capabilities resulting from the application of dynamic control systems may be limited. It is thus essential that a target or an obstacle be detected and located at a minimum distance of about 1000

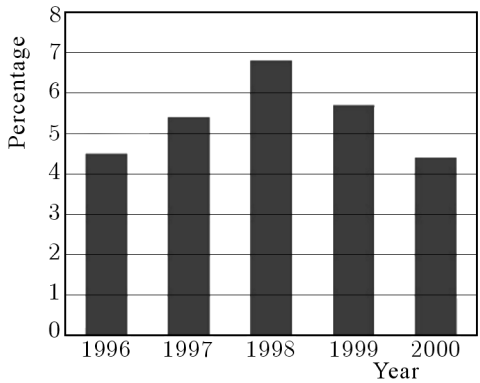

Fig. 3. Collisions with power lines involving commercial helicopters in percentage % in the US between 1996 and 2000; the total number of accidents being 934 (Monsoo Park, 2003)

meters. Design engineers are looking for more and more sensitive measurement instruments that remain unaffected by disturbance signals coming from various technological devices.

In modern warfare scenarios, military aircraft are used for a number of different tasks including destruction and paralysis of targets emitting electromagnetic fields. Examples of such targets include radiolocation stations and radio/television transmission stations emitting high-frequency signals as well as high-voltage power lines, power stations or substations emitting low-frequency signals. Under warfare conditions, such objects are usually protected against destruction, so it is essential that they be attacked with smart munitions. In each case, a successful attack requires precise detection, location and guidance.

If an overhead high-voltage transmission line or a similar object is to be attacked, the target detection process commences when an onboard monitoring device receives a 50 Hz-frequency signal. A complete operation of target location requires such data as the direction of the signal emission and the distance between the target and the monitoring device. The latter can be established basing, for instance, on the target voltage. It is relevant to know the exact distance if the target is attacked by means of a missile equipped with a warhead detonated by a preprogrammed time fuze. However, if the attack is performed automatically after the target is approached, it is sufficient to know the target direction. The warhead is detonated once the signal confirming the missile position in the direct or indirect zone is received.

The work discusses the principles of location of angular positions of point targets using the example of overhead power lines as well as the guidance of an air-attack aircraft. Special attention is paid to the reduction of disturbance signals by employing active filters and a gyroscope-based stabilizer.

2. Detection and location of the angular position of a point target

Transmission lines as well as certain ground elements of a power network emit 50 Hz electric and magnetic fields. The intensity of the electric field is constant in time; it is proportional to the electric voltage in the element or line. It is dependent on the distance from the field source and on configuration of screening elements, e.g. earthed structures, transmission towers, etc.

The intensity of magnetic field is proportional to the intensity of the corresponding electric current flow. The field changes along with changes in the current. The intensity of the electric and magnetic fields decrease considerably when the distance from the radiation source increases. Similar phenomena are observed when an aerial vehicle moves away from the axis of a transmission line or approaches a lattice-type pylon acting as a screen. Buildings, trees or bushes found in the vicinity of a transmission line may also act as screens; nonetheless, they hardly ever affect the readings, because an object is detected, tracked and attacked from an altitude higher than the top of pylons or other sources emitting the low-frequency electric field.

The preliminary tests described in detail in Szmitkowski *et al.* (2003) were conducted under static conditions. The results show that the closer the measurement sensor is to the ground, the smaller is the intensity of the electric field (Fig. 4). Then, the accuracy of the measurement system was analysed under motion conditions with the aim of determining the effect of disturbance signals. The measurements were performed at certain distances from the line where the signals were still measurable under static conditions. During the tests, the system encountered problems. The low-frequency disturbances that occurred at the output were difficult to specify, and their amplitude was higher than that of useful signals. This resulted from the high-speed motion and the vibrations of the measurement system. At a distance of approximately 60 meters from a 100 kV high-voltage line, the disturbance amplitude was nearly 100 times higher than the amplitude of the useful signal.

It can be concluded that low-frequency disturbance voltage of the order of several to several dozen Hz induced in the sensor can be due to the rapid crossing through the Earth's magnetic field lines.

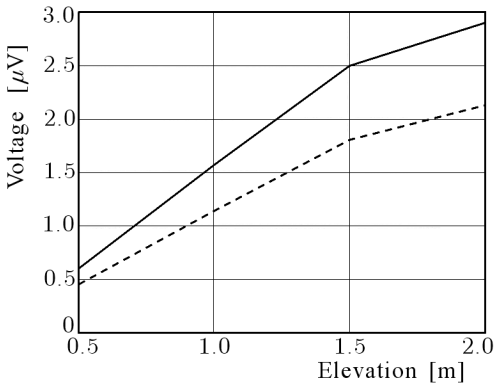

Fig. 4. Graph exemplifying the relationship between the sensor output voltage and the elevation (110 kV-power line, solid line – distance of 20 m, broken line – distance of 40 m) (Szmitkowski *et al.*, 2003)

Moreover, during the in-motion tests, the system was susceptible to disordered disturbances in form of electrostatic discharges, which were attributable to friction between the system casing and the cloth as well as friction between the casing and the air stream coming out of the nozzle. The latter type of disturbances can occur if the system is fitted on board of a flying object.

The disturbance signals with frequencies other than 50 Hz, which is characteristic for useful signals, can be reduced by using active filters. Preliminary tests show that there is still one more type of interference that cannot be reduced by means of electric methods. The signal at the output of the measuring system is greatly dependent on the angle of sensor inclination in relation to the horizontal plane (Fig. 5).

The intensity of an electric field is dependent on the voltage but independent of the current flowing through the system; therefore, it is assumed that the electric field intensity can be used for the detection of a target. The target is detected when the on-board monitoring system receives a 50 Hz signal from an active high-voltage line or some other element of a power network found at a certain distance. In order to accurately locate a point target, it is necessary to know the direction from which the emitted signal comes as well as the distance from the monitoring system.

The study involved developing and constructing directional sensors, measurement amplifiers with amplification of more than 10^6, and systems of high-pass filters with high goodness-of-fit suitable for filtering low-frequency disturbances. The filters possess very sharp amplitude characteristics and very narrow pass bands (Tuśno and Koruba, 2008).

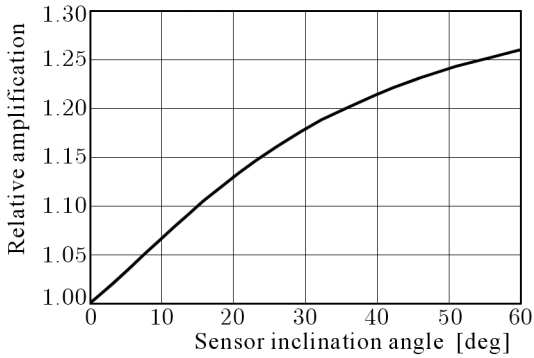

Fig. 5. Relative change in voltage induced at the sensor output in function of the angle of sensor inclination with respect to the horizontal plane (measurements at a distance of 30 m from a 15 kV-power line) (Koruba and Tuśno, 2008)

The principle of target detection and location is presented schematically in Fig. 6 (Tuśno and Koruba, 2006). A point target emitting an electromagnetic field E is inside the right angle formed by the axes of two directional sensors. Each sensor consists of a high-inductivity coil wound around a ferrous rod. A 50 Hz alternating voltage signal induced at each sensor needs to be amplified, filtered with band-pass filters to eliminate disturbance signals and then rectified with an ideal rectifier (AC/DC converter). Voltages u_1 and u_2 are measured and processed along twin measurement paths, Tp_1 and Tp_2, by applying the principles described below.

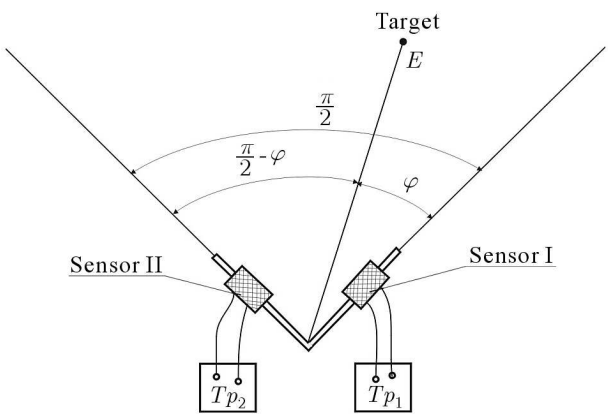

Fig. 6. Schematic diagram of the concept for locating the angular position of a point target (Tuśno and Koruba, 2006)

In Tuśno and Koruba (2006), a relationship was derived to combine the voltages u_1 and u_2 at the sensor outputs with the angle of target deflection φ from the axis of sensor 1

$$\frac{u_1}{\cos\varphi} = \frac{u_2}{\sin\varphi} \;\Rightarrow\; \frac{u_2}{u_1} = \frac{\sin\varphi}{\cos\varphi} = \tan\varphi \tag{2.1}$$

The above relationship shows that it is possible to determine the angular position of the point target in the system presented in Fig. 2 by measuring voltages at the outputs of the sensors lying perpendicularly to each other and determining their quotient. The instantaneous value of angle φ can be established by performing the operation

$$\varphi = \arctan\frac{u_2}{u_1} \tag{2.2}$$

If the bisector of the angle measured between the axes of the two sensors coincides with the axis of the aerial vehicle flying towards the target as well as the line of sight, then we have

$$\varphi = \frac{\pi}{4} = \arctan 1 \tag{2.3}$$

In this case, the maintaining of the flight path towards the target requires keeping the angle $\varphi = \pi/4$ constant. Thus, it is necessary that the voltages at the two measurement paths be the same, and that their quotient, u_2/u_1, be equal to 1.

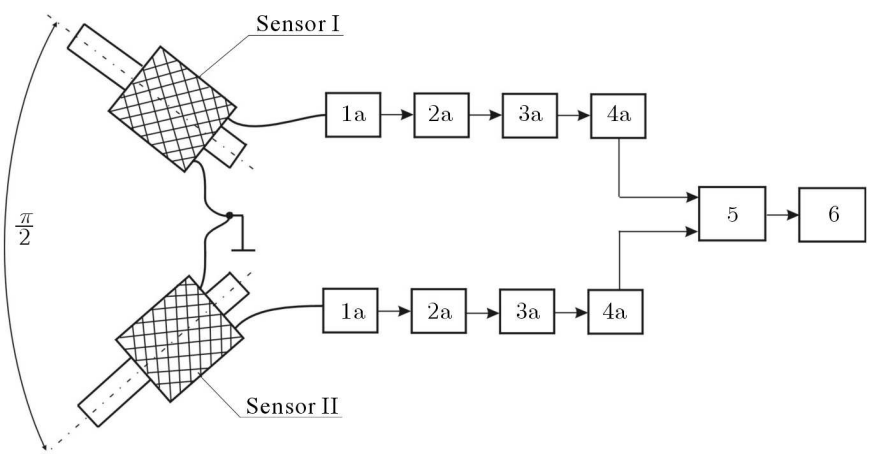

Fig. 7. A block diagram of the point-target location system (Tuśno and Koruba, 2008)

Figure 7 shows a block diagram of a system capable of locating a point target in a part of a plane limited by the lines of the sensor axes. In the system, the paths of amplifiers and filters are identical. Voltages generated at the outputs of the directional sensors are provided to initial measurement amplifiers, 1a and 1b, with amplification of above 10^6. In order to eliminate electric disturbances and to select useful signals, it is necessary to supply the initially amplified signals to two systems of band-pass filters, 2a and 2b, with a medium frequency of 50 Hz. It is required that the filters possess a very sharp characteristic and a narrow pass band. The tests involved using systems of the 8-th order Butterworth filters with a goodness-of-fit Q, equal to 10 (Tuśno and Koruba, 2007). After filtration, the signals in both measurement paths are amplified in final amplifiers, 3a and 3b, and then rectified in ideal full-wave rectifiers, 4a and 4b. Another functional block is unit 5 dividing the signals from the measurement paths (performing the operation $y = u_2/u_1$). The quotient undergoes conversion in functional generator, 6, realising the initial function, in accordance with relationship (2.2).

3. The concept of a gyroscope-based system for stabilising sensors positions

The positions of sensors are stabilised by a gyroscope with three degrees of freedom.

Applying Fig. 8 and assuming that the rotor is an axially symmetric body, we can omit the frame inertia. Moreover, since the high-speed rotational velocity is constant and the gyroscope is of the astatic type (where the mass centre coincides with the centre of both frames), the equations of motion of the gyroscope axis can be written as follows (Koruba and Osiecki, 2006)

$$\begin{aligned} &J_{gk}\frac{d\omega_{gy_3}}{dt} - J_{gk}\omega_{gx_2}\omega_{gz_3} + J_{go}n_g\omega_{gz_3} = M_b - M_{rb} \\ &J_{gk}\frac{d}{dt}(\omega_{gz_2}\cos\vartheta_g) - (J_{go}\dot{\omega}_{gx_2} + J_{gk}\omega_{gy_1}\omega_{gz_2})\sin\vartheta_g + \\ &\quad -J_{go}n_g(\omega_{gy_1} + \dot{\vartheta}_g)\cos\vartheta_g + J_{gk}\omega_{gy_2}\omega_{gx_1} = M_c - M_{rc} \end{aligned} \tag{3.1}$$

where

$$\begin{bmatrix} \omega_{gx_1} \\ \omega_{gy_1} \\ \omega_{gz_1} \end{bmatrix} = \begin{bmatrix} p^*\cos\psi_g + q^*\sin\psi_g \\ -p^*\sin\psi_g + q^*\cos\psi_g \\ \dot{\psi}_g + r^* \end{bmatrix}$$

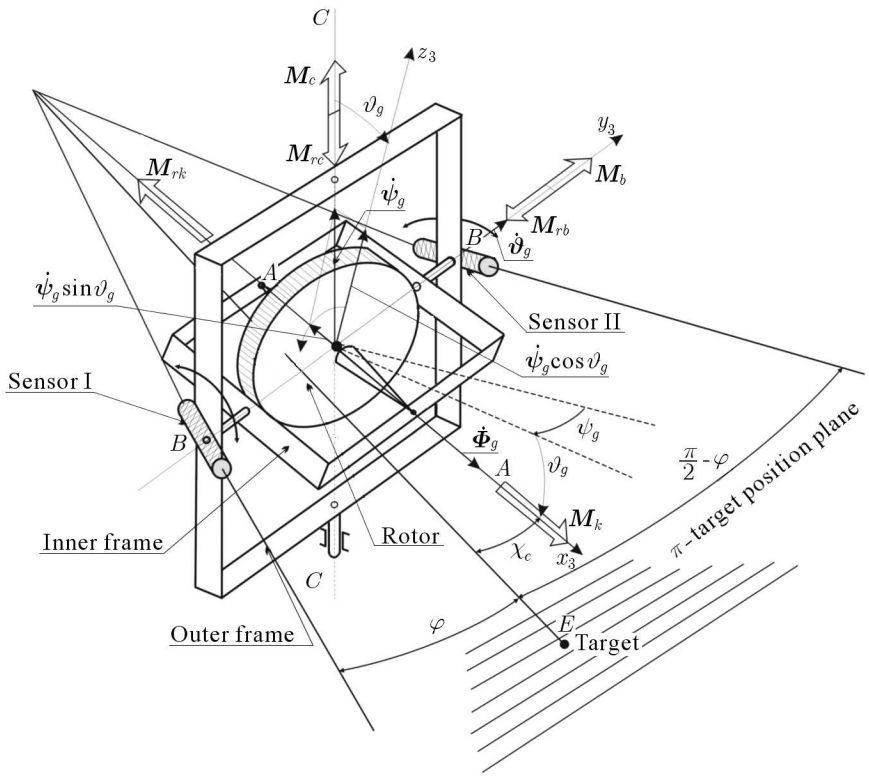

Fig. 8. View of the sensors arrangement in a controlled gyroscope with the assumed coordinate systems

$$\begin{bmatrix}\omega_{gx_2}\\ \omega_{gy_2}\\ \omega_{gz_2}\end{bmatrix} = \begin{bmatrix}(p^*\cos\psi_g + q^*\sin\psi_g)\cos\vartheta_g - (r^* + \dot{\psi}_g)\sin\vartheta_g\\ -p^*\sin\psi_g + q^*\cos\psi_g + \dot{\vartheta}_g\\ (p^*\cos\psi_g + q^*\sin\psi_g)\sin\vartheta_g + (r^* + \dot{\psi}_g)\cos\vartheta_g\end{bmatrix}$$

$$\begin{bmatrix}\omega_{gx_3}\\ \omega_{gy_3}\\ \omega_{gz_3}\end{bmatrix} = \begin{bmatrix}(p^*\cos\psi_g + q^*\sin\psi_g)\cos\vartheta_g - (r^* + \dot{\psi}_g)\sin\vartheta_g + \dot{\Phi}_g\\ -p^*\sin\psi_g + q^*\cos\psi_g + \dot{\vartheta}_g\\ (p^*\cos\psi_g + q^*\sin\psi_g)\sin\vartheta_g + (r^* + \dot{\psi}_g)\cos\vartheta_g\end{bmatrix}$$

and

J_{go}, J_{gk} – moments of inertia of the gyroscope rotor moving about its longitudinal and transverse axes, respectively

ϑ_g, ψ_g – angles determining the position of the gyroscope axis in space (angles of rotation of the inner and outer frames, respectively)

n_g – angular velocity of the gyroscope rotation

p^*, q^*, r^* – components of the vector of the gyroscope base rotational velocity
M_k – moment of the force driving the gyroscope rotor
M_{rk} – moment of friction forces acting on the rotor bearings in the inner frame and the aerodynamic drag
M_b, M_c – moments of forces controlling the inner and outer frame, respectively
M_{rb}, M_{rc} – moments of friction forces in the bearings of the inner and outer frame, respectively.

The sensors are rigidly fixed to the inner frame so that they are perpendicular to each other in the frame plane (Fig. 5). This allows stable positioning of the sensors irrespective of the gyroscope base movements. The sensors may not maintain their predetermined position in the desired plane because of external disturbances, friction in the suspension bearings, frame inertia, nonlinearity of gyroscope motion, or the Earth's spin. It is essential to apply additional correction moments to minimize the effect of disturbances and, in consequence, to maintain the gyroscope axis in the desired position. The algorithm for changes in the correction moments can be written as (Koruba and Osiecki, 2006)

$$M_b = -k_b\vartheta_g + k_c\psi_g - h_g\frac{d\vartheta_g}{dt}$$
$$M_c = -k_c\vartheta_g - k_b\psi_g - h_g\frac{d\psi_g}{dt} \tag{3.2}$$

where
k_b, k_c – coefficients of amplifications of the gyroscope corrector
h_g – coefficients of damping of the gyroscope corrector.

4. Controlling the gyroscope during location of a point source of electromagnetic radiation from board of an aerial vehicle

The task requires knowing the dynamic properties of the attack vehicle as well as the characteristics of the measurement system responsible for detecting and locating the target position. A special strategy needs to be applied so that the detection, tracking, guiding and attack are performed with precision. Targets such as transmission lines or substations are usually disabled by means of graphite bombs, which work by spreading a cloud of conductive composite

filaments. If a flying object is to attack a target that is linear in character, e.g. a transmission line, the flight path needs to be optimised and the target has to be reached with as many clusters as possible. The first cluster reaching a power line disables it, so the other clusters become incapable of tracking it any more.

In a general case, the controlled air attack weapon is a multidimensional object of regulation. An aerial vehicle used for destroying ground elements of a power network needs to have at least two quantities regulated: altitude and the angle of deflection from the line of sight. Changes in altitude do not affect the angle of deflection considerably. The cross-coupling causes such a small error that it can be neglected.

The angle of deflection of the object from the target path can be regulated by using relationships (2.2) and (2.3) and by assuring that $u_2/u_1 = 1$. This is the case of automatic regulation when the target is tracked along the shortest path. Moreover, it seems possible to regulate the process by applying the difference $u_2 - u_1 = 0$ as the desired value. This method could simplify the design of the control system considerably by replacing the dividing system (Fig. 3) with a simple differential amplifier. Another advantage of this method is the fact that at larger distances from the target, the error values are small, and the regulation is smoother. The closer to the target, the more rapid the increase in the intensity of the electric field, the higher the value of the error, and the more rapid the response.

Figure 9 shows a simplified schematic diagram of the guidance control of an aerial vehicle approaching electromagnetic radiation emitted by a fixed point ground target. The position of the point ground target (PGT) emitting electromagnetic radiation in relation to the aerial vehicle (AV), i.e. the target line of sight (LOS), can be determined from the following equations (Koruba and Osiecki, 2006)

$$\begin{aligned}
\frac{dr}{dt} &= -V_b[\cos(\varepsilon - \gamma_b)\cos\sigma\cos\chi_b + \sin\sigma\sin\chi_b] \\
\frac{d\sigma}{dt} &= \frac{V_b[\cos(\varepsilon - \gamma_b)\sin\sigma\cos\chi_b - \cos\sigma\sin\chi_b]}{r} \\
\frac{d\varepsilon}{dt} &= \frac{V_b\sin(\varepsilon - \gamma_b)\cos\chi_b}{r\cos\sigma}
\end{aligned} \tag{4.1}$$

Let us demand that the AV is guided towards the PGT using the method of proportional navigation, i.e.

$$\frac{d\chi_b}{dt} = a_\chi\frac{d\sigma}{dt} \qquad \frac{d\gamma_b}{dt} = a_\gamma\frac{d\varepsilon}{dt} \tag{4.2}$$

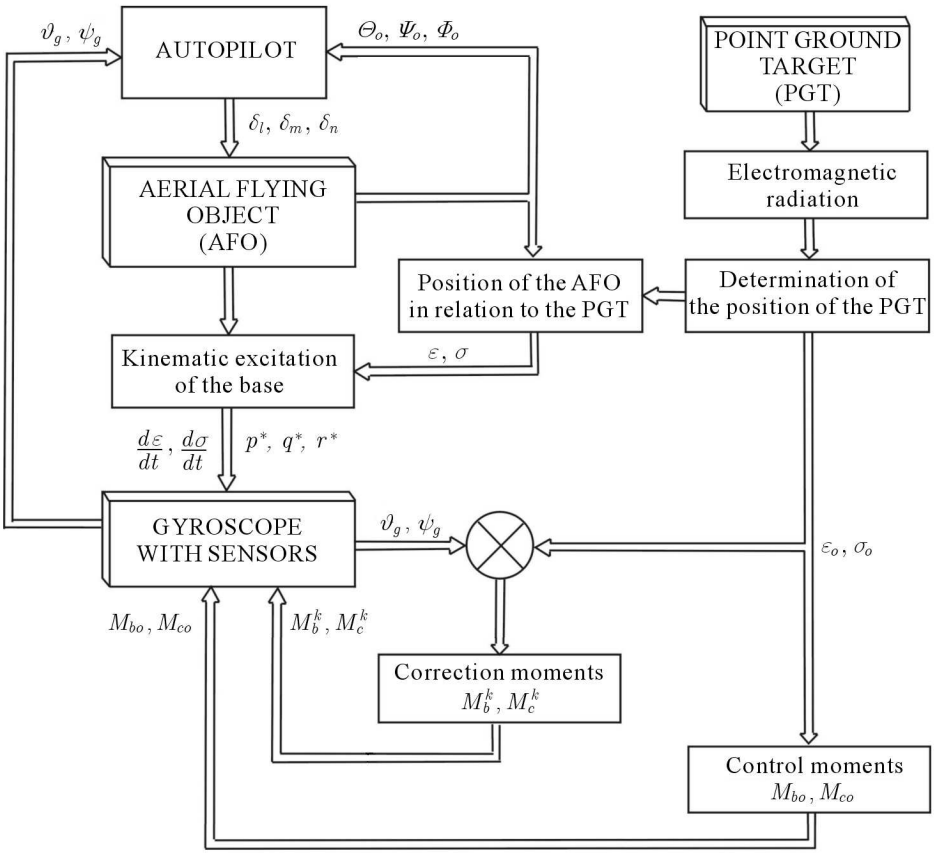

Fig. 9. A schematic diagram of the guidance of an aerial vehicle approaching a point ground target emitting electromagnetic radiation

where a_χ, a_γ are coefficients of proportional navigation.

The initial conditions of the distance between the AV and PGT are

$$r_o = \sqrt{(x_{bo} - x_{co})^2 + (y_{bo} - y_{co})^2 + (z_{bo} - z_{co})^2}$$
$$\sigma_o = \arcsin \frac{y_{co} - y_{bo}}{r_o} \qquad \varepsilon_o = \arctan \frac{z_{bo} - z_{co}}{x_{co} - x_{bo}} \tag{4.3}$$

where

- r – distance between the AV and the PGT
- ε, σ – angles determining the position of the AV in space
- V_b – flight velocity of the AV
- γ_b, χ_b – angles determining the orientation of the vector of flight velocity of the AV in space

r_o – initial distance between the AV and the PGT (on detection of the PGT)

ε_o, σ_o – angles determining the initial position of the LOS in space (on detection of the PGT)

x_{bo}, y_{bo}, z_{bo} – initial position of the AV in space (on detection of the PGT)

x_{co}, y_{co}, z_{co} – position of the PGT.

The controlled mechanical gyroscope equipped with sensors fitted to its inner frame is the executive element responsible for determination the line of sight, that is the position of the point grounded target (PGT). The gyroscope axis should coincide with the bisector of the right angle created by the two sensors axes (Fig. 9). The task of the gyroscope automatic control system is to change the position of the high-speed rotation axis so that it shows the point with the highest radiation intensity (target) and coincides with the line of sight (LOS). As a result, the value of the angle $\varphi = \pi/4$ will remain constant, thus the voltages in the two measurement paths will be equal and their quotient will be $u_2/u_1 = 1$. The control moments applied to the gyroscope frames should change in accordance with the law (Koruba, 2001)

$$\begin{aligned} M_b &= -k_b(\vartheta_g - \varepsilon) + k_c(\psi_g - \sigma) - h_g\Big(\frac{d\vartheta_g}{dt} - \frac{d\varepsilon}{dt}\Big) \\ M_c &= -k_c(\vartheta_g - \varepsilon) - k_b(\psi_g - \sigma) - h_g\Big(\frac{d\psi_g}{dt} - \frac{d\sigma}{dt}\Big) \end{aligned} \tag{4.4}$$

The problem to be solved is to make the gyroscope axis coincide with the line of sight once the target is detected. If there is a high discrepancy in the initial conditions, the gyroscope axis may deflect from the predetermined direction significantly. The system of automatic control can generate controls that will turn out to be technically unfeasible or will cause a loss in the gyroscope stability.

In order to make the gyroscope axis coincide with the LOS, it is necessary to apply appropriate moments of control force to the gyroscope frames (Koruba, 1999). The best solution would be to demand that the gyroscope axis being in a given initial position $\vartheta_g(t_o) = \vartheta_{go}$ and $\psi_g(t_o) = \psi_{go}$ be set at: $\vartheta_{go}(0) = \varepsilon_o$ and $\psi_{go}(0) = \sigma_o$ by means of $M_{bo} = \text{const}$ and $M_{co} = \text{const}$. From this position, the moments M_b and M_c, determined and described by expressions $(3.1)_2$, will maintain the gyroscope axis in the desired path, i.e. along the line of sight. Thus, we control the gyroscope axis in two steps. First, we apply constant moments, and then we apply moments described by equations $(3.1)_2$ as soon as $\vartheta_g = \varepsilon_o$ and $\psi_g = \sigma_o$.

Under the initial conditions, where $\ddot{\vartheta}_{go} = 0$, $\dot{\vartheta}_{go} = 0$, $\ddot{\psi}_{go} = 0$, and $\dot{\psi}_{go} = 0$, we solve the simplified linear equations (Koruba, 2001)

$$\begin{aligned}\vartheta_g(t) &= \vartheta_{go} + \frac{\Omega(\eta_c M_{bo} + M_{co})}{J_{gk}\omega_{go}^2}\Big[t - \frac{2h_g^*}{\omega_{go}^2}\Big(1 - \mathrm{e}^{-h_g^* t}\cos(\omega_g^* t)\Big) + \\ &- \frac{(\omega_g^*)^2 - (h_g^*)^2}{\omega_{go}^2\omega_g^*}\mathrm{e}^{-h_g^* t}\sin(\omega_g^* t)\Big] \\ \psi_g(t) &= \psi_{go} + \frac{\Omega(\eta_b M_{co} - M_{bo})}{J_{gk}\omega_{go}^2}\Big[t - \frac{2h_g^*}{\omega_{go}^2}\Big(1 - \mathrm{e}^{-h_g^* t}\cos(\omega_g^* t)\Big) + \\ &- \frac{(\omega_g^*)^2 - (h_g^*)^2}{\omega_{go}^2\omega_g^*}\mathrm{e}^{-h_g^* t}\sin(\omega_g^* t)\Big]\end{aligned} \tag{4.5}$$

where

$$\omega_g^* = \sqrt{\omega_{go}^2 - (h_g^*)^2} \qquad \omega_{go}^2 = (1 + \eta_b\eta_c)\Omega^2$$
$$h_g^* = \frac{\Omega}{2}(\eta_b + \eta_c) \qquad \Omega = \frac{J_{go}n_g}{J_{gk}}$$

At the first stage of calculation, an approximation technique can be applied for high values of h_g^* and a short time of motion

$$\vartheta_g(t) \approx \vartheta_{go} + \frac{\Omega(\eta_c M_{bo} + M_{co})}{J_{gk}\omega_{go}^2}t \qquad \psi_g(t) \approx \psi_{go} + \frac{\Omega(\eta_b M_{co} - M_{bo})}{J_{gk}\omega_{go}^2}t \tag{4.6}$$

Now, it is necessary to select the time in which the gyroscope axis moves from the position ϑ_{go}, ψ_{go} to position $\vartheta_g = \varepsilon_o$, $\psi_g = \sigma_o$. Let us denote the time by t_g. Then, from the above approximated equalities we get

$$\vartheta_{go} + \frac{\Omega(\eta_c M_{bo} + M_{co})}{J_{gk}\omega_{go}^2}t_g = \varepsilon_o \qquad \psi_{go} + \frac{\Omega(\eta_b M_{co} - M_{bo})}{J_{gk}\omega_{go}^2}t_g = \sigma_o \tag{4.7}$$

It is a system of two equations with two unknowns: M_{bo} and M_{co}. Hence

$$\begin{aligned}M_{bo} &= \frac{\eta_b(\varepsilon_o - \vartheta_{go}) + J_{go}n_g(\sigma_o - \psi_{go})}{t_g} \\ M_{co} &= \frac{\eta_c(\sigma_o - \psi_{go}) - J_{go}n_g(\varepsilon_o - \vartheta_{go})}{t_g}\end{aligned} \tag{4.8}$$

If the gyroscope axis is to be moved from the known initial position ϑ_{go}, ψ_{go} to the desired position, where it coincides with the line-of-sight, in the time t_g, then the control moments, M_{bo} and M_{co} described by Eqs. (4.8) need to be applied to the inner and outer frames of the gyroscope. After the time t_g, the gyroscope is controlled according to the algorithm described by formulas (4.4).

5. Discussion of results

To illustrate the process of stabilisation of the sensor position in a desired plane, let us consider an example of computer simulation conducted for the following data

$$J_{gk} = 2.5 \cdot 10^{-4}\ \text{kgm}^2 \qquad J_{go} = 5.0 \cdot 10^{-4}\ \text{kgm}^2$$
$$n_g = 1000\ \text{rad/s} \qquad \eta_b = \eta_c = 0.01\ \text{Nms}$$

The correction coefficients for the gyroscope corrector are optimally determined taking into consideration the minimum mean-square error (Koruba and Osiecki, 2006). It is assumed that $k_b = 10$, then other coefficients can be calculated as follows

$$k_c = \frac{1}{2}\frac{J_{go}^2 n_g^2}{J_{gk}}\sqrt{2J_{go}^2 n_g^2 + 4J_{gk}k_b}$$
$$h_g = \sqrt{2J_{go}^2 n_g^2 + 4J_{gk}k_b}$$

It is also assumed that the sensors are in the predetermined horizontal plane, i.e. the frames are set at the following angles $\vartheta_{go} = 0$ and $\psi_{go} = 0$. The gyroscope base undergoes harmonic angular displacements in the vertical and horizontal planes: $Q = Q_o \sin(\nu t)$, $R = R_o \cos(\nu t)$, respectively. As a result, the angular velocities will be: $q^* = Q_o \nu \cos(\nu t)$ and $r^* = -R_o \nu \sin(\nu t)$, respectively.

Moreover, it is assumed that $Q_o = 0.5\,\text{rad}$, $R_o = 0.25\,\text{rad}$ and $\nu = 5\,\text{rad/s}$, and that the displacement occurs at $t_p = 1.0\,\text{s}$ and lasts till $t_k = 3.0\,\text{s}$. Let us analyse what effect the above disturbances have on the gyroscope stability. Figure 10 shows the influence of disturbance displacement on stabilisation of the sensor position at various values of the coefficient of friction in the gyroscope frame bearings. Figure 11 presents the gyroscope axis paths at various values of the coefficient of friction in the gyroscope frame bearings.

Figure 12a illustrates the effectiveness of the method of disturbance reduction by applying the correction moments M_b and M_c. Figure 12b confirms that the concept of the stabilisation system with sensors fitted to the gyroscope frames is feasible.

Figures 13-16 show selected results of computer simulation of the gyroscope control by applying sensors of electromagnetic radiation. The gyroscope is responsible for determination of the line-of-sight in such a way that an aerial guided bomb moves towards the target along the path presented in Fig. 13, according to the proportional navigation method with the coefficients $a_\chi = 3.5$

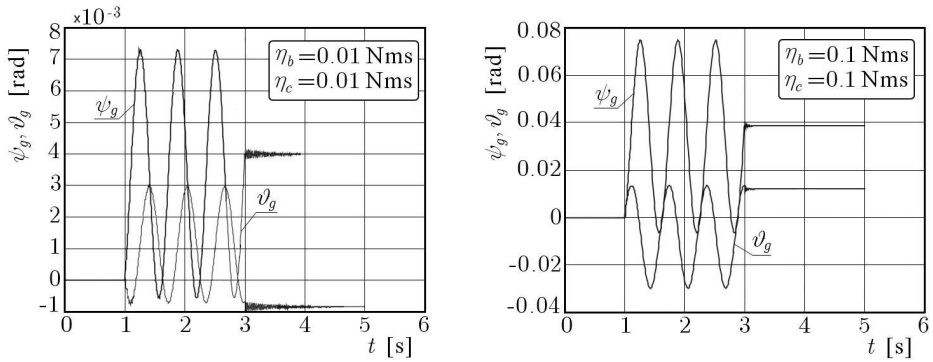

Fig. 10. Time-dependent changes in angles of deflection of the gyroscope frames ϑ_g and ψ_g at (a) low and (b) high coefficients of friction in the frame bearings

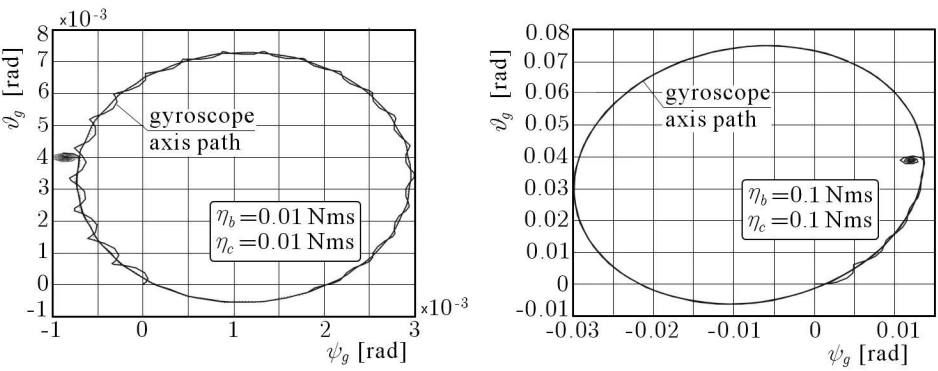

Fig. 11. Gyroscope axis paths at (a) low and (b) high coefficients of friction in the frame bearings

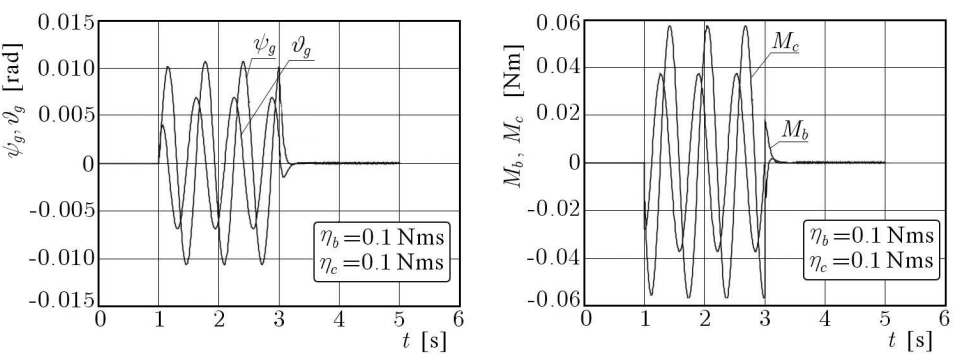

Fig. 12. Time-dependent changes (a) in angles ϑ_g and ψ_g of the gyroscope frame deflections following the application of the correction moments M_b and M_c, and (b) in the correction moments M_b and M_c

and $a_\gamma = 3.5$. Figure 14 shows the desired angles σ_o and ε_o as well as the actual angles ψ_g and ϑ_g of the gyroscope position axis in function of time in an open-loop mode of control. The accuracy of the control operation is greatly affected by friction in the frame bearings. Figure 15 illustrates the effect of external disturbances on the gyroscope operating in the open- and closed-loop modes. Thus, if the coefficients of friction in the frame bearings are high, the external disturbances will cause considerable deflections of the gyroscope axis from the desired position. Correction controls reduce these deflections to a minimum. As can be seen from Fig. 15, the program and correction controls, M_{bo}, M_{co} and M_b and M_c, respectively, do not reach high values, so they can be applied technically.

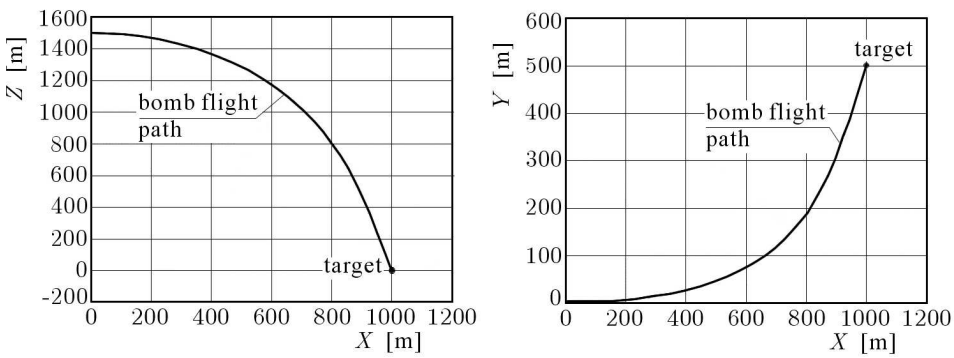

Fig. 13. Bomb flight paths (a) in the vertical plane and (b) in the horizontal plane

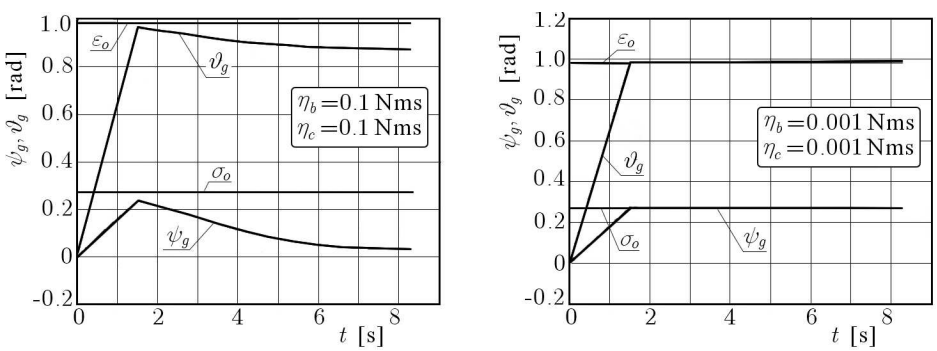

Fig. 14. Controlling the position of the gyroscope axis (LOS) at (a) high and (b) low coefficients of friction in the bearings of the gyroscope frames

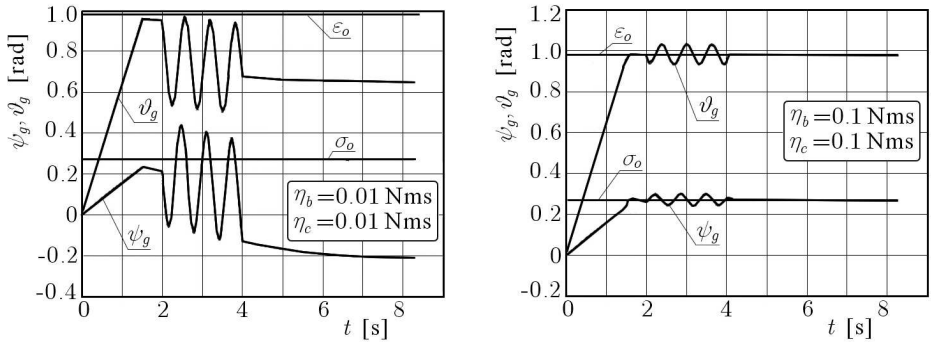

Fig. 15. Controlling the position of the gyroscope axis (LOS) affected by disturbances with the gyroscope operating in (a) an open-loop mode (b) a closed-loop or back coupling mode

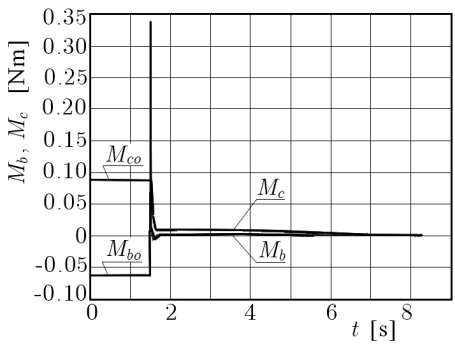

Fig. 16. Program and correction controls of the AV gyroscope in time, M_{bo}, M_{co} and M_b, M_c, respectively

6. Conclusion

The preliminary analysis confirms that the gyroscope-based system for stabilising the angular position of onboard sensors can be efficiently employed to detect and locate overhead high-voltage power lines. As the base of the mechanical gyroscope with three degrees of freedom, i.e. the board of the aerial vehicle, is affected by considerable disturbances, the stabilisation process requires application of correction moments.

The work also considers the applicability of the gyroscope-based system to the guidance of an aerial vehicle towards a point target emitting low-frequency electromagnetic radiation. The gyroscope performance accuracy greatly affects the precision of target location and the homing operations in the case of a fixed point ground target emitting electromagnetic radiation.

The advantages of the gyroscope-based system include simplicity and a low cost, but first and foremost, reliability and stability while guiding an AV under conditions of external disturbances.

The results of computer simulations and experiments conducted under laboratory conditions are positive. The method may turn out to be very efficient for the guidance of selected types of weapon of precise-destruction, e.g. guided bombs and unmanned aerial vehicles.

Acknowledgement

The authors acknowledge support from the Polish Ministry of Science and Higher Education through Project 0N514001534 of the 2008-2010 education budget.

References

1. Koruba Z., 1999, The inverse problem of dynamics in a control system based on a free gyroscope to be used in an unmanned aerial vehicle, *The Bulletin of the Military University of Technology on Flight Physics and Aircraft Armament*, Warsaw, **557**

2. Koruba Z., 2001, *Dynamics and Control of an Onboard Gyroscope Used in Unmannned Aerial Vehicles*, Monographs, Studies and Dissertations, No. 25, Kielce University of Technology, Kielce, p. 285

3. Koruba Z., Osiecki J.W., 2006, *The Design, Dynamics and Navigation of Selected Precision-Destruction Weapons*, Course book, Kielce-University-of-Technology Publishing House, ISBN 83-88906-17-8, p. 484

4. Koruba Z., Tuśnio J., 20o8, Gyroscope as a stabilizer of the angular position of onboard sensors for detecting and locating overhead high-voltage power lines, *Measurement Automation and Robotics*, **2**, 763-772

5. Monsoo Park, 2003, *Millimeter-Wave Polarimetric Radar Sensor for Detection of Power Lines in Strong Clutter Background*, Dissertation for the degree of Doctor of Philosophy in University of Michigan

6. Szmitkowski J., Tuśnio J., et al., 2003, *A Method and Equipment for Monitoring the Hazard of Electrocution During Rescue Operations*, A research project report, The Main School of Fire Service, Warsaw

7. Tuśnio J., Koruba Z., 2006, A concept for determining the angular position of a low-frequency electromagnetic radiation source using the example of overhead power network structures, *6th International Armaments Conference*, Waplewo

8. TUŚNIO J., 2006, Detecting and locating electric power network structures, *Preceedings of the 2nd International Conference on Scientific Aspects of Unmanned Aerial Vehicles*, Kielce-Cedzyna

9. TUŚNIO J., KORUBA Z., 2007, Generation and reduction of slow-varying disturbances affecting the operation of systems for detection and Location of electromagnetic fields from overhead power lines, *8th Conference on Active Noise and Vibration Control Methods MARDiH*, Kraków-Krasiczyn, Poland, ISBN 83-89772-41-8

10. TUŚNIO J., KORUBA Z., 2008, Target location and guidance of an attack aircraft towards a source of low-frequency electromagnetic radiation, *Measurement, Automation and Robotics*, **2**, 783-792

Giroskopowy układ lokalizacji punktowego źródła promieniowania elektromagnetycznego małej częstotliwości

Streszczenie

W opracowaniu przedstawiono koncepcję, model matematyczny oraz szacunkowe obliczenia dotyczące lokalizacji położenia kątowego punktowych urządzeń elektroenergetycznych. Rozpatrywana jest także możliwość naprowadzania obiektu latającego na tego rodzaju urządzenia.

Manuscript received November 21, 2008; accepted for print December 29, 2008